島根大学地質学研究報告　14, 1～14ページ（1995年12月）
Geol. Rept. Shimane Univ., 14, p. 1～14 (1995)

An integrated evaluation of the mechanical behaviour of normally consolidated cohesive soils

Takeshi Kamei*

Abstract

This paper describes an integrated study of the mechanical behaviour of normally consolidated cohesive soils, by means of a series of triaxial tests on cohesive soils covering a wide range of plasticity index, and centrifuge model tests on failure of embankments constructed on cohesive soils.

Results of the triaxial tests show that strength anisotropy and strain anisotropy become more marked for soils with a lower plasticity index. In the centrifuge test, significant lateral deformation due to embankment loading was observed in soil with a low plasticity index. In addition, an attempt was made to provide likely explanations by Finite Element Method analysis. The numerical method proposed in this paper is a simple procedure which predicts with sufficient accuracy, the actual deformation of a deep clay foundation under embankments, although a number of simplifing assumptions have been made in terms of the soil parameters and deformation analyses. It is concluded that this method can be used as a preliminary design in engineering practice.

Key words: cohesive soil, consolidated undrained shear, constitutive equation of soil, deformation, finite element method, plasticity, soft ground, triaxial test

Introduction

It has been several decades since geotechnical researchers developed the finite element method (FEM) and centrifuge modelling techniques. Most researchers who are familiar with both techniques would agree that they should be developed as complementary approaches to performance for predicting prototype behavioural phenomenon with any real confidence. In essence, if a high-confidence numerical solution to a geotechnical analysis or design problem cannot be obtained, centrifuge modelling should be considered (Mitchell, 1991). Geotechnical engineers, on the other hand, encounter a variety of soils on the construction site, from gravel to clay. Naturally engineering properties of these soils vary according to the grain distribution.

In engineering practice, natural soils have intermediate properties between cohesive soils and cohesionless soils. This group of soils has been named the intermediate soils (Osterberg, 1978). Engineering questions are i) What kind of soil indices and what value of these indices should be used to classify soils into the two groups? ii) How reliable and economical are polarized design procedures? iii) Are normal geotechnical problems adequately solved by the application of elemental testing and numerical analyses? Answers to all of the above questions involve an understanding of the behaviour of cohesive soils. There is a need for an appropriate technology for deformation characteristics of clay foundation. Such a technology must be practical, low cost to employ, and have a theoretical basis.

Several attempts have been made to correlate engineering properties of soils to simple soil indices. A good example is the Skempton's empirical equation (1957) which relates the ratio of undrained shear strength (c_u) to effective overburden pressure p' to plasticity index. Such correlations play an important role in practice by providing estimates of parameter values for use in preliminary design, and serve as a check on data obtained from laboratory and in-situ tests.

Kurata and Fujishita (1961) carried out various tests on artificially mixed soil samples. Their work provided a basis for a design code to classify soils into the two

* Department of Geosciense, Shimane University, 1060 Nishikawatsu, Matsue 690, Japan.

groups for marine construction work in Japan. Similar tests were carried out by Nakase and Kamei (1983) on reconstituted soil samples prepared by mixing the Kawasaki marine clay with the Toyoura sand and its crushed portion. In this series of tests, the plasticity index was selected for specifying the soil type, considering the importance of this index in geotechnical engineering.

The experimental results showed that the undrained shear strength anisotropy increased with decreasing plasticity index, and that soils with plasticity indices between 15 and 20 were considered the intermediate soils in view of the shape of stress paths and degree of the strength anisotropy (Nakase and Kamei, 1983).

A large testing programme to study the mechanical characteristics of soils with a wide range of plasticity index from 10 to 55 was carried out by Kamei (1985). The twelve soils tested were obtained from various places along the coastal areas of Japan. Based on the test data, Kamei (1985) proposed linear correlations between some soil parameters and plasticity index. Consistency of data from the clay–sand mixtures and natural clays suggested that the undrained shear characteristics of natural clays could be extrapolated from results obtained on clay–sand mixtures only. It would be interesting to investigate the possible deformation behaviour of embankment foundations using constitutive equations of soils.

However, the costs, time, facilities and required expertise are often not available within the constraints of practical engineering work, particularly for small projects. In these situations, the greatest benefits of sophisticated new analytical methods are to be derived from the results of convenient studies which have been reduced to a simple form.

The purpose of this paper is to investigate the mechanical behaviour of normally consolidated cohesive soils, and to facilitate the selection of suitable analytical techniques for the geotechnical engineer concerned with deformation analysis of clay foundations under embankments. A series of element tests, centrifuge modelling tests on embankment failures, and Finite Element Method analysis have been investigated. The applicability of a simple method proposed by the author to predict the deformation characteristics of the foundation during embankment construction are reviewed and discussed.

Soils tested and testing programme

The Kawasaki clay mixture series used in this series of experiments is composed of five soils named M–10, M–15, M–20, K–30 and K–50. The numbers refer to their plasticity index (PI), and the M prefix stands for mixture. K–30 and K–50 were dredged samples of the Kawasaki clay, whereas M–10, M–15 and M–20 were clay–sand mixtures. K–30 Kawasaki clay was used as the base material to formulate the clay–sand mixture soils by adding different amounts of commercially available Toyoura sand. To obtain a smooth grading, some amounts of crushed particles of Toyoura sand which contain about 15% of silt were also added to the mixture. The preparation method for such soil samples has been reported in detail elsewhere (Nakase and Kamei 1983; Kamei 1985; Nakase et al. 1988).

Grain size distribution curves and the plasticity chart of the samples suggest that the artificially mixed soils are similar to marine clays found in the coastal areas of Japan. There is evidence from triaxial and oedometer tests that mechanical characteristics of Kawasaki clay–mixture series correspond well to that of reconstituted natural marine clays having the same PI (Kamei 1985; Nakase and Kamei 1988; Nakase et al. 1988). Thus, Kawasaki clay–mixture series can be used to assess the mechanical behaviour of reconstituted natural cohesive soils.

Stress–strain characteristics

Figure 1 shows typical stress–strain curves of K–30 and M–10 in the CKoU tests, where the principal stress difference $q=\sigma_a-\sigma_r$ is normalized by the vertical effective consolidation pressure σ_{vc}'. The anisotropy in the stress–strain characteristics has been summarized as follows; i) the maximum principal stress difference of compression loading is larger than that of extension loading....anisotropy in strength, ii) the axial strain at failure is smaller than that of extension loading.... anisotropy in strength mobilization, and iii) in contrast to elastoplastic behaviour in compression loading, in extension loading there is bilinear behaviour with an inflection point occuring near the point where the orientation of the principal stress changes....anisotropy in stress–strain behaviour.

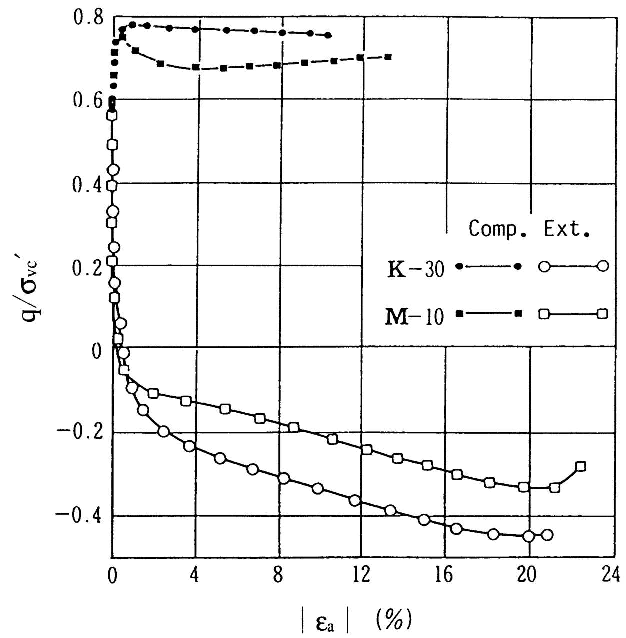

Fig. 1 Typical stress–strain curves of K–30 and M–10 in Ko–consolidated specimens (Nakase and Kamei, 1983).

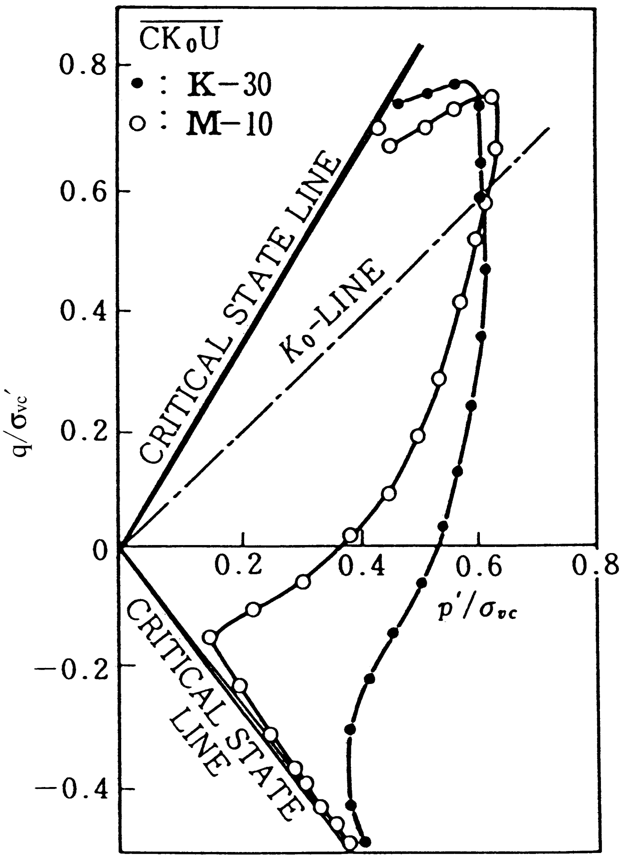

Fig. 2 Normalized effective stress paths in p′: q space (Nakase and Kamei, 1983.)

The same data used to produce the stress–strain curves are replotted in p′: q stress, normalized by the vertical effective consolidation pressure σ_{vc}', where p′=the mean effective stress; and q is the principal stress difference as seen in Fig.2. The undrained effective stress path forms a portion of the yield surface. As seen in Fig.2, the yield surface becomes flatter with decreasing plasticity index. In other words, the magnitude of excess pore pressure built up due to the change in deviatoric stress becomes larger for soils having a smaller plasticity index.

The ratio of axial strains extension and compression loadings is plotted against Ip in Fig.3, where failure is defined as the point of maximum principal stress difference. As seen in this figure, the ratio of axial strains at failure increases sharply with a decrease in Ip. For soils with Ip more than 20 which corresponds to general marine clays, the axial strain at failure by the extension loading is about 20 to 30 times that by the compression loading. And for soils with Ip=10, it reaches 80 times.

Figure 4 shows typical stress ratio η(=q/p′)–axial strain curves of the Ko–consolidated specimens, where the stress ratio is normalized by dividing by the η at maximum principal stress difference. The important points in this figure are: i) failure in compression loadings on M–10 occurs at a very small axial strain of about 0.25% which is about 1/3 of that for K–30, and ii) the stress ratio η in extension loadings at the axial strain equal to that at failure of compression loading remains positive. The reciprocal of $\eta/\eta_{at(\sigma_1-\sigma_3)max}$ may be considered a measure of the safety factor against shear failure. Figure 4 may imply, therefore, that when the safety factor in the compressive failure is unity, the safety factor in the extension side is about 5 for K–30 and infinite for M–10. Anisotropy in strength mobilization also increases with a decrease in Ip. To illustrate the influence of anisotropy in element test on ground deformation, the case of a surface loaded foundation (Fig.5) is considered. The soil mass beneath the loading zone, is an active zone (in a compressive state) and the behavior against loading is rigid–plastic (see Fig.1). The engineering significance of the point is that in the compression loadings, the development of a slip line can be observed clearly in the ground at the point of incipient failure.

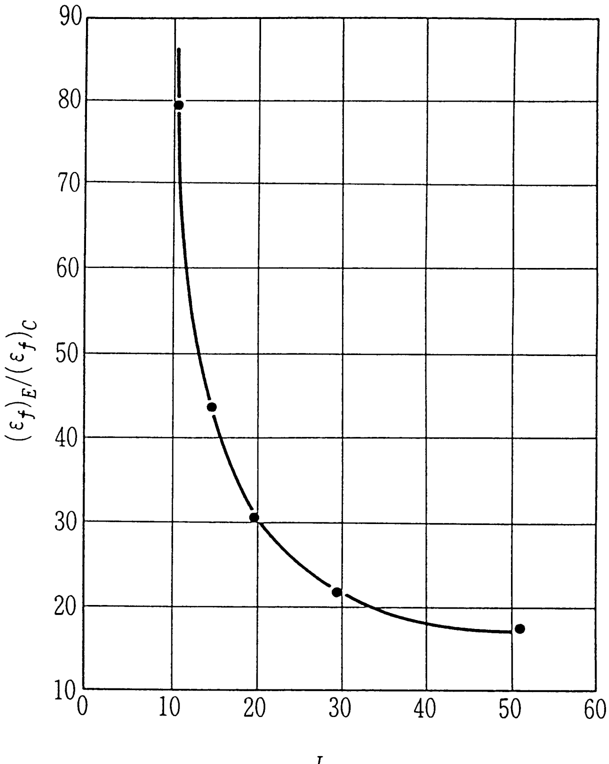

Fig. 3 The ratio of the axial strain at failure of extension and compression loadings plotted against PI.

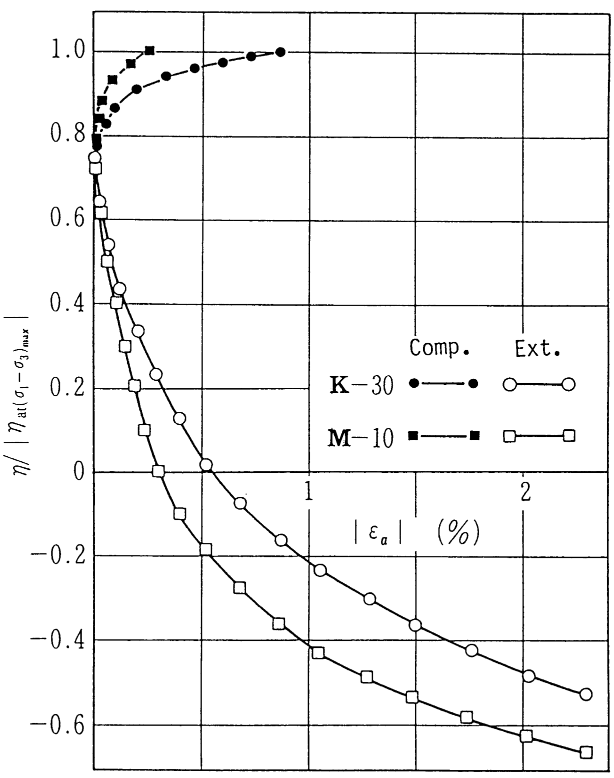

Fig. 4 Typical stress ratio $\eta/\eta_{at(\sigma_1-\sigma_3)max}$ – strain curves of K–30 and M–10 in Ko–consolidated specimens.

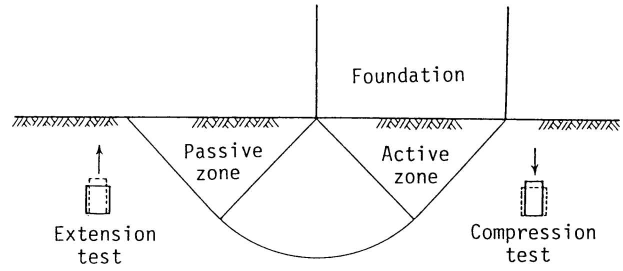

Fig. 5 Typical failure mechanism in the case of a surface loaded foundation.

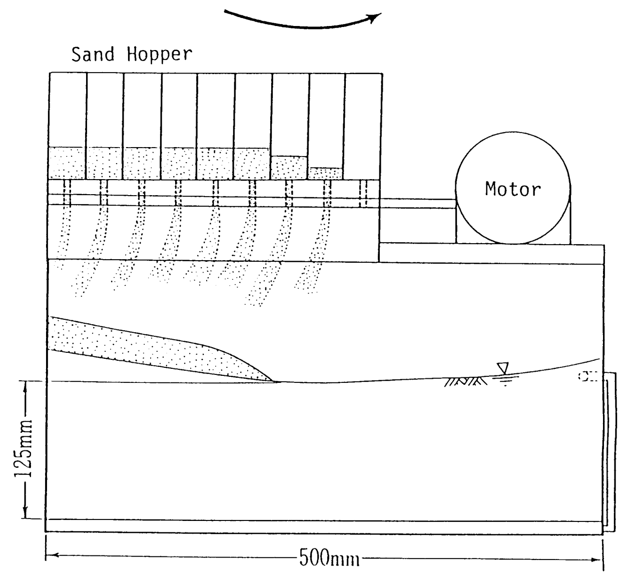

Fig. 6 The method of embankment construction used.

However, in the passive zone outside the loading zone, the soil mass is in the extensive state. Even if the strain in the active zone reaches that of compressive failure, it is still much smaller than the strain needed to fail the soil in the passive zone as seen in Fig.1. Accordingly, the slip line cannot be clearly observed in passive zone. In addition, it is expected that this trend becomes more marked for soils with a lower plasticity index as seen in Figs. 2 to 4.

Centrifuge model test

In order to investigate the difference in ground deformation corresponding to a change in plasticity index, centrifuge model tests on failure of embankments constructed on soils with M–10 and K–30 have been conducted (Naganuma et al., 1983).

The method for constructing an embankment in an operating in a centrifuge test package has been developed

Table 1 A set of soil parameters estimated by plasticity index (PI)

Soil Parameters	r
$\lambda = 0.02 + 0.0045 \cdot PI$	0.98
$\kappa = 0.00084 \cdot (PI - 4.6)$	0.94
$N = 1.517 + 0.019 \cdot PI$	0.95
$M_C = 1.65$	—
$M_E = 1.385 - 0.00505 \cdot PI$	0.85
$K_{ONC} = 0.45$	—
$K_{OOC} = K_{ONC} \cdot (OCR)^{0.45}$	—
$v' = K_{ONC} / (1 + K_{ONC})$	—
$k_v = k_{v0} \cdot \exp\{(e - e_0)/\lambda_k\}$	—
$\lambda_k = 0.073 + 0.019 \cdot PI$	0.98

r : coefficient of correlation in linear regession analyses

by Fukuda (1983), which is very similar to that described by Basset and Horner (1979). Figure 6 illustrates the test system used.

Embankments were constructed in a two-dimensional steel package which has a transient plate on one side and a sand hopper located inside. The sand embankment is constructed by pouring sand from the hopper while the centrifuge is continuously in motion. There is a series of small holes in both the bottom plate of the sand hopper and the sliding plate. The sliding plate is driven by a reversible motor until the position of the small holes in the two plates overlap. The sand then starts pouring from the sand hopper.

After the completion of preconsolidation on the laboratory floor (1 g), the package was installed in the centrifuge apparatus and brought to the state of consolidation by self weight. During and after the construction, the pore pressures were continuously recorded by a magnetic tape recorder, which traced the development of consolidation. After dissipation of excess pore pressure, the sand embankment wasconstructed by pouring sand from the sand hopper while the centrifuge was continuously in motion, and the ground was brought to the point of failure.

The loading term was unable to be controlled in the present system, because of self-dropping of sand particles. However, the depth of ground which started to drain during, the loading term could be calculated by assuming that the one-dimensional consolidation isochrones might be approximated by parabolas (Schofield and Wroth, 1968). Estimated depths were about 2 mm for K-30 ground, and 5 mm for M-10 ground. The observed failure of ground was significantly deeper than

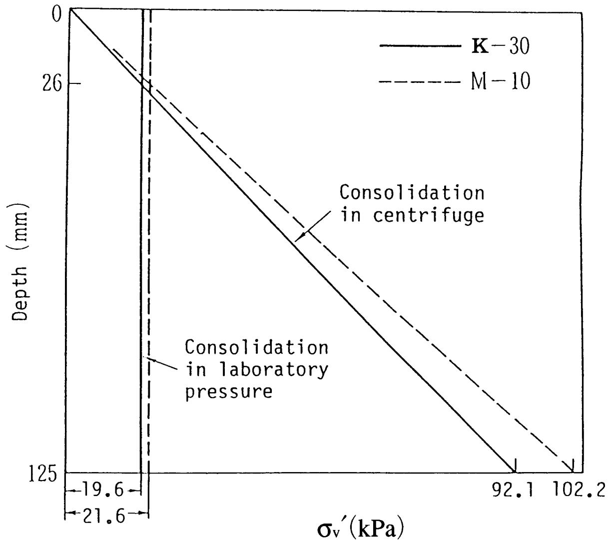

Fig. 7 Distribution of vertical effective stress with depth.

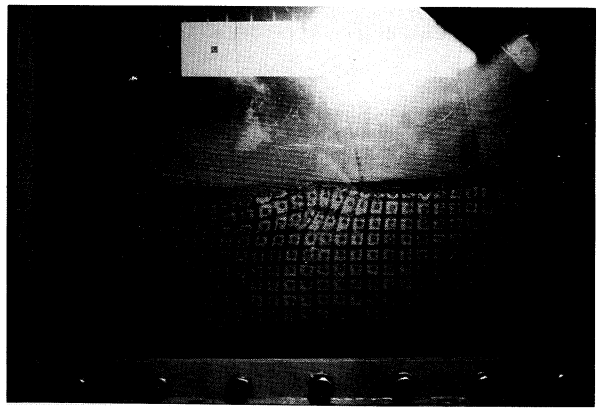

Photo. 1 K-30 ground at failure.

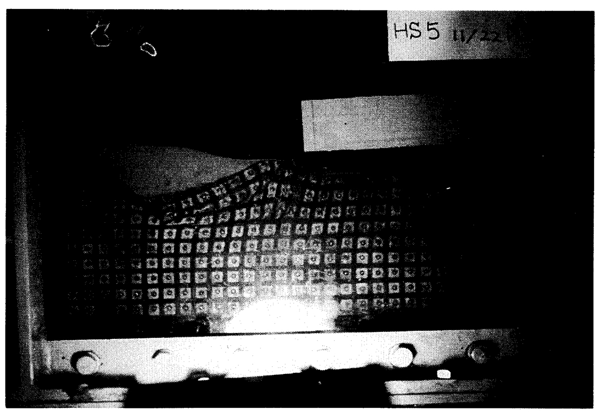

Photo. 2 M-10 ground at failure.

these values, therefore, the loading was probably carried out under undrained conditions.

Both ground types were set to have the same value of undrained compressive strength, in order for easy comparison of anisotropy in the ground. This was achieved by adjusting the centrifugal acceleration and preconsolidation pressure, considering the submerged unit weight and the c_u/p value which was obtained by Ko–consolidated plane strain undrained compression loading tests. The values of preconsolidation pressure and centrifugal acceleration used in the present experiment are shown in Table 1. The resulting distribution of vertical effective stress with depth is as shown in Fig.7.

Figure 8 shows the displacement vector at failure for the K–30 ground observed in the experiment, and Photograph 1 shows the K–30 ground at failure. A clear slip line was observed in the active zone. The failure can be considered as a rotational mechanism of a rigid body, as shown by the displacement vectors. For the passive zone, however, no obvious slip line was observed. This observation agrees with the prediction based on the anisotropy observed in element tests, i.e., the different response to the external force between compression and extension loadings. Furthermore, the important point in the K–30 ground is that the deformation below the slip line is very small and the slip line has become a distinct discontinuity of the velocity field. Figure 9 shows the displacement vector at failure for the M–10 ground observed in the experiment, and Photograph 2 shows the M–10 ground at failure. The slip line of the M–10 ground is shallower than that of the K–30 ground, and was not clearly observed in the passive part. Looking at deformation of the M–10 ground as a whole, significant deformation was observed outside the slip line and the deformation zone progressed more deeply than the K–30 ground. This result agrees with that predicted from the deformation modulus anisotropy that has been previously described in detail elsewhere (Nakase and Kamei, 1984).

It is likely that a slip failure occured during the time interval of 2 seconds for photographing, and the

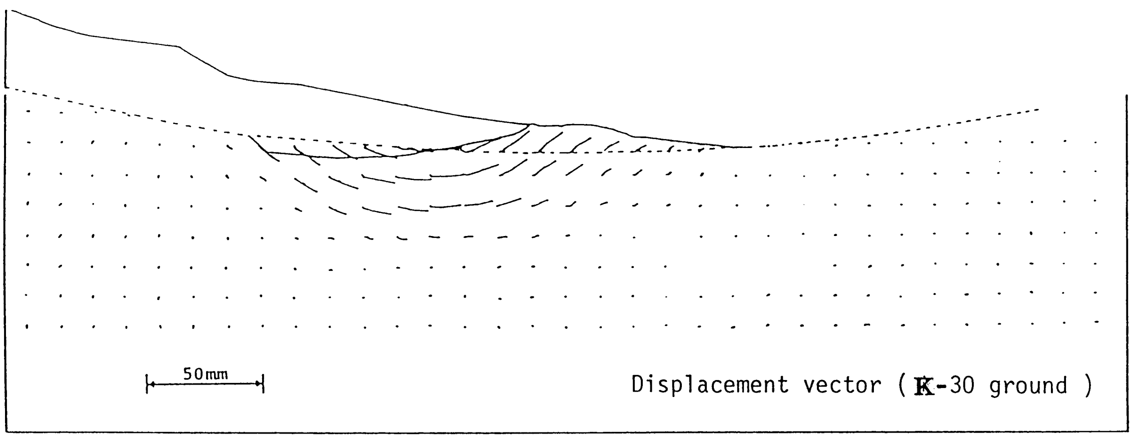

Fig. 8 Deformation vector at failure for K–30 ground.

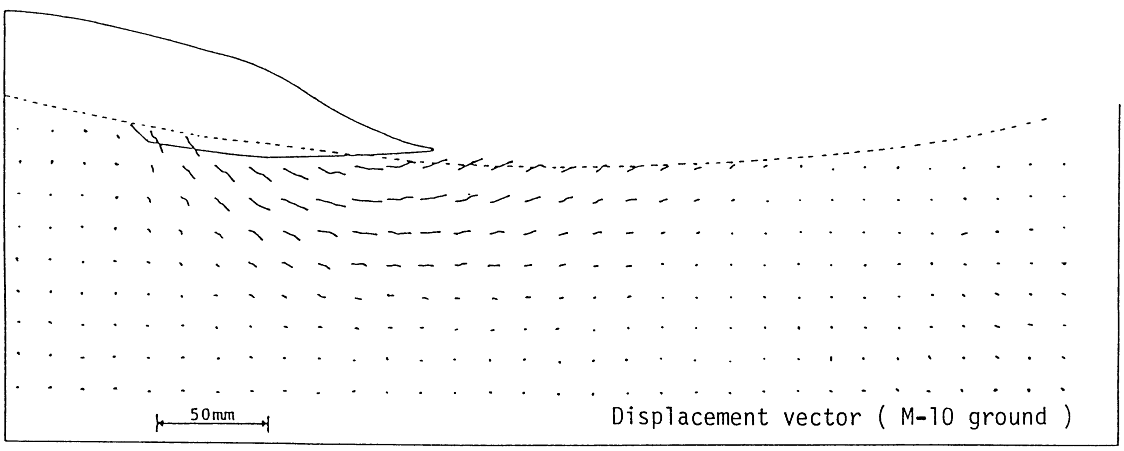

Fig. 9 Deformation vector at failure for M–10 ground.

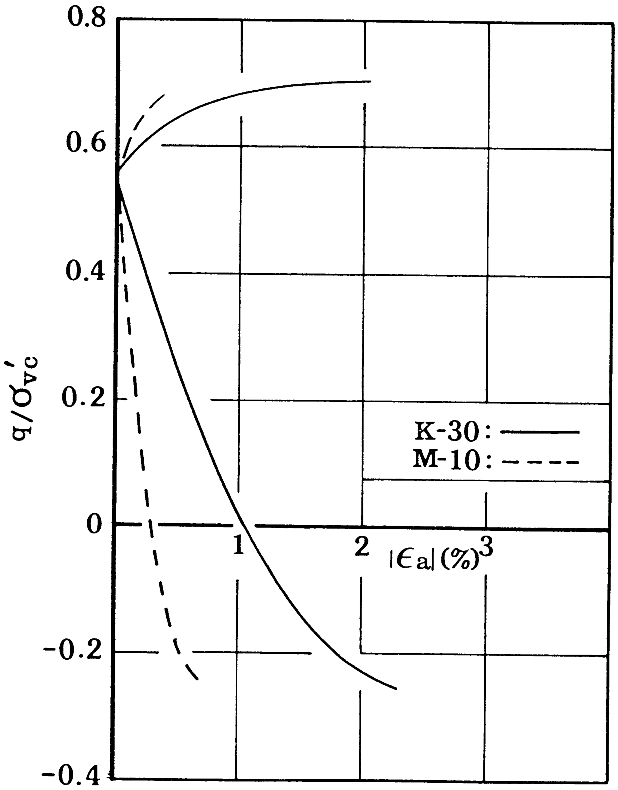

Fig. 10 Stress–strain curves of Sekiguchi–Ohta model estimated by present correlations (Nakase et al., 1988).

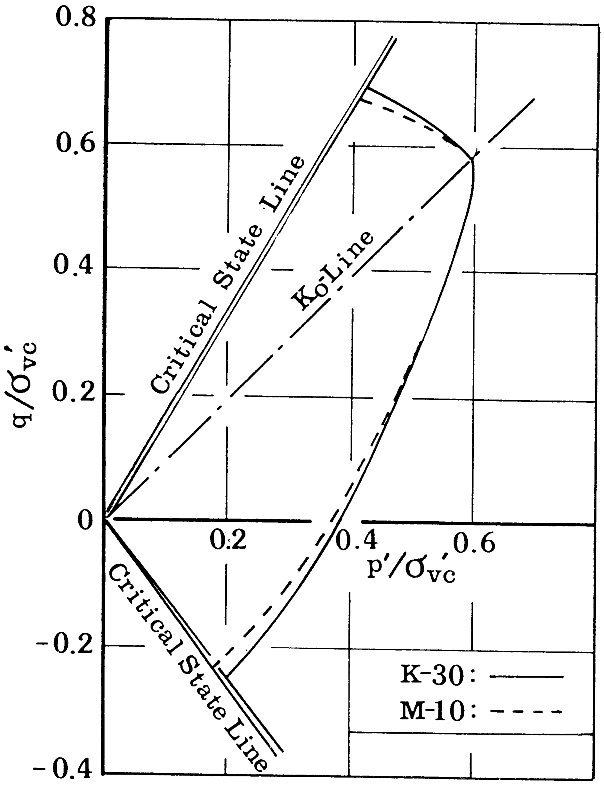

Fig. 11 Effective stress paths of Sekiguchi–Ohta model estimated by present correlations (Nakase et al., 1988).

deformation was further increased because of the increase in embankment loading. Therefore, it cannot be confirmed at present that the observed difference in the deformation zone is due solely to the difference in soil type.

It is observed that, at the edge of the embankment, the direction of the displacement vector is horizontal for the M–10 ground and 45 degrees upwards for the K–30 ground. This means that lateral deformation is pronounced in the ground with a lower plasticity index. In the present experiment, both materials have an identical distribution of compressive strength in the vertical direction. Results of the element test show that the undrained shear strength initiated by extension loading decreases to about 50% of that by compression loading for soils with Ip=10. These seem to explain the difference in the two ground types.

Judging from the centrifuge model test results of failure mechanism in the ground, a clear slip line in the active part due to anisotropy, was observed. This results

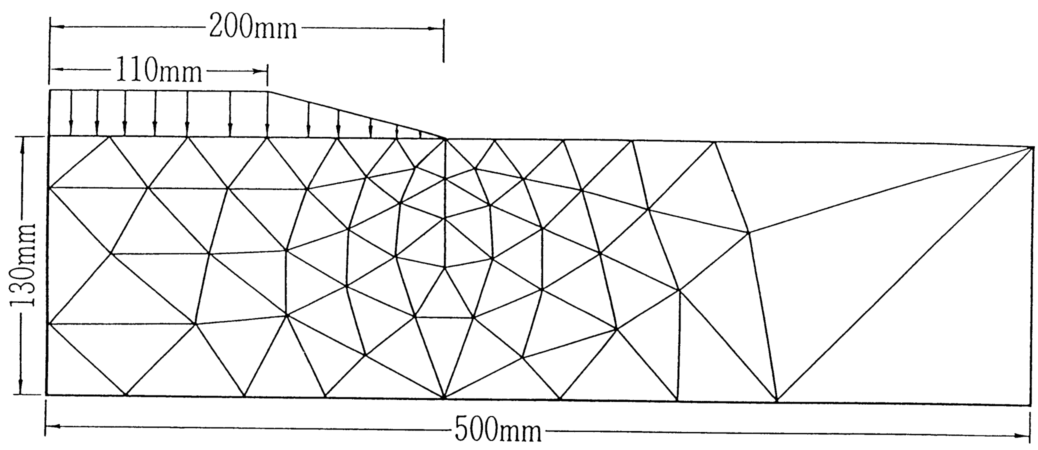

Fig. 12 The Finite Element Method mesh used in the present computation.

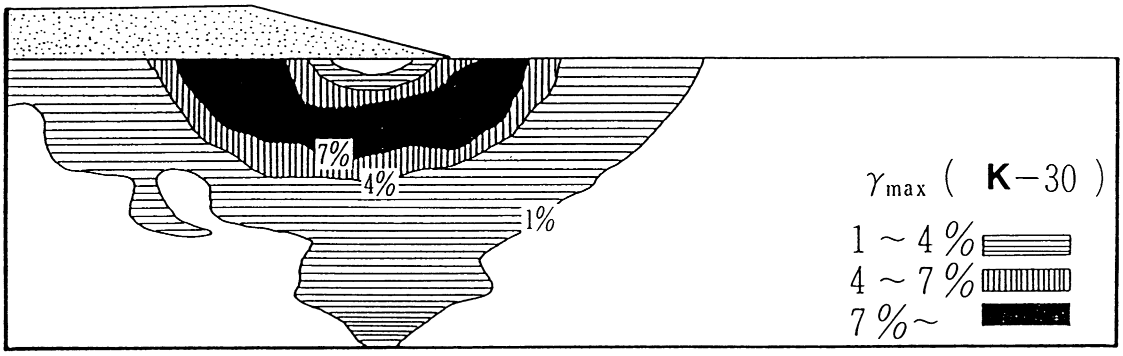

Fig. 13 Contour of maximum shear strain for K–30 ground.

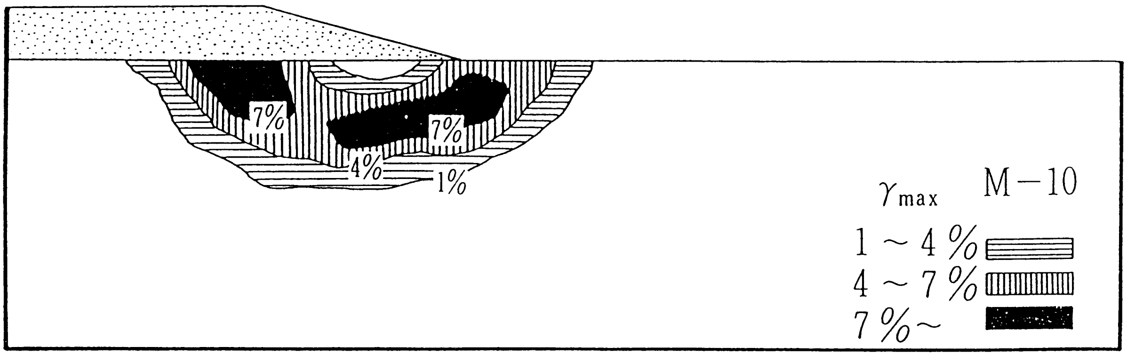

Fig. 14 Contour of maximum shear strain for M–10 ground.

in a field of discontinuous line and the deformation does not progress below the slip line. For the passive part, however, such a line was not observed. This is due to the anisotropy in the strength mobilization. These observations compare well with the element test results on anisotropy.

In the present experiment, although a degree of anisotropy in the ground due to the difference in plasticity index cannot be clearly confirmed, no slip line was observed in the passive part of K–30 ground. Significant lateral deformation due to embankment loading was observed in soil with a plasticity index of 10.

Numerical analysis

A large testing program, consisting of triaxial compression, triaxial extension, and oedometer tests on twelve prepared soils has been performed (Kamei, 1985 ; Nakase et al.,1988 ; Kamei and Sakajo,1993). The soils exhibited a wide range in plasticity index, from 10 to 55. These tests were performed to study whether it is possible to determine parameters specific to a constitutive soil model simply by using the plasticity index. Linear correlations between the soil parameters for constitutive equations and the plasticity index were obtained with high values noted in the coefficients of correlation as shown in Table 1. It may be appropriate to demonstrate the overall accuracy of the relationships obtained from this series of tests by calculating stress–strain curves and stress paths for two different soils (K–30 and M–10) subjected to Ko–consolidation and having different values of plasticity index. Numerical illustrations to check the overall accuracy of the correlations were also developed.

The stress–strain curves for the two soils are shown in Fig.10, where mobilization of strength starts at the smallest axial strain for the soil having the smallest value of PI, without regard to the shearing direction. This is consistent with the observed experimental data shown in Fig.1. Figure 11 shows the two effective stress paths. Although the Sekiguchi–Ohta model cannot predict the latter part of the stress paths, the numerical example well illustrates features of the stress paths, where the yield surface becomes flatter with decreasing plasticity index(Nakase et al.,1988). These two figures clearly demonstrate that the relationships deduced from the experimental data can be used to estimate soil parameters of the constitutive equations by using PI.

Boundary conditions, stress state and soil parameters are well defined in this model test. Finite element analysis was,therefore, performed by using the Sekiguchi–Ohta model with anisotropic consolidation but neglecting the cohesive effect(Sekiguchi and Ohta,1977). The finite element mesh used in this calculation is shown in Fig.12: the element is an isoparametric triangle element. In the analysis, an undrained condition is considered by assuming the compressive coefficient of water is 100 times that of soil skeleton.

The contour of the maximum shear strain obtained by the F.E.M. analysis, performed by the use of experimental soil parameters for the K–30 and M–10 grounds are shown in Figs.13 and 14. The result of the F.E.M. analysis corresponds well to experimental observation for the K–30 ground. However, significant lateral deformation, which is a characteristic of M–10 ground, is not shown by this analysis.

Evaluation of deformation characteristics of deep clay foundations under embankments using the proposed correlations

Sakajo and Kamei(1995) investigated whether it was possible to estimate the mechanical behaviour of clay foundations under embankments using an elasto–plastic model proposed by Sekiguchi and Ohta(1977) and constitutive parameters estimated by plasticity index proposed by Kamei(1985) and Kamei and Sakajo(1993), and, if so, how accurate these predictions are. The results obtained by Sakajo and Kamei(1995) to check the applicability of the proposed method to the fields are briefly reviewed.

The trial embankment construction was done in the Kanda district of the Joban Expressway in Ibaraki Prefecture near Tokyo, Japan(Japan Highway Public Corporation and Fudo Construction Co., Ltd.,1981; Sekiguchi et al., 1984). The cross section of the Kanda Trial Embankment foundation is shown in Fig.15. The embankment was constructed on a 25.9 m deep cohesive soil deposit(silt layers are deposited at depths of 23.3 m to 25.9 m, as shown in Fig.16). The natural water content of the soil is almost the same value as its liquid limit. This cohesive soil stratum, therefore, is in a normally consolidated state. All soil parameters estimated by plasticity index(PI) are shown in Table 2. The finite Element Method used in the study is shown in Fig.17.

The settlement of the ground surface and the excess pore pressure are shown relative to elapsed time in Figs.18 and 19 respectively. Figs.20(a) and (b) show the computed ground deformation at the completion of the embankment construction and at 300 days passed since the commencement of embankment construction, respectively. Reasonable agreements have been obtained between the measured and the computed values of the settlement and the excess pore pressure for the soil layers quantitatively. In addition, the ground surface movements beneath the centre and beneath the shoulder of the embankment can be shown qualitatively. The analytical results obtained by the proposed method(Kamei

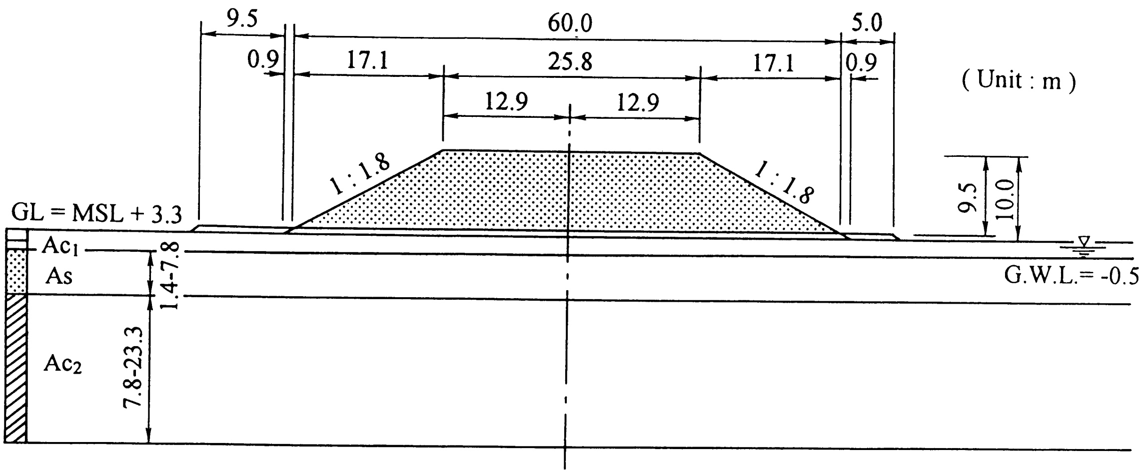

Fig. 15 Cross section of the Kanda Trial Embankment foundation(Japan Highway Public Corporation and Fudo Construction Co., Ltd.,1981).

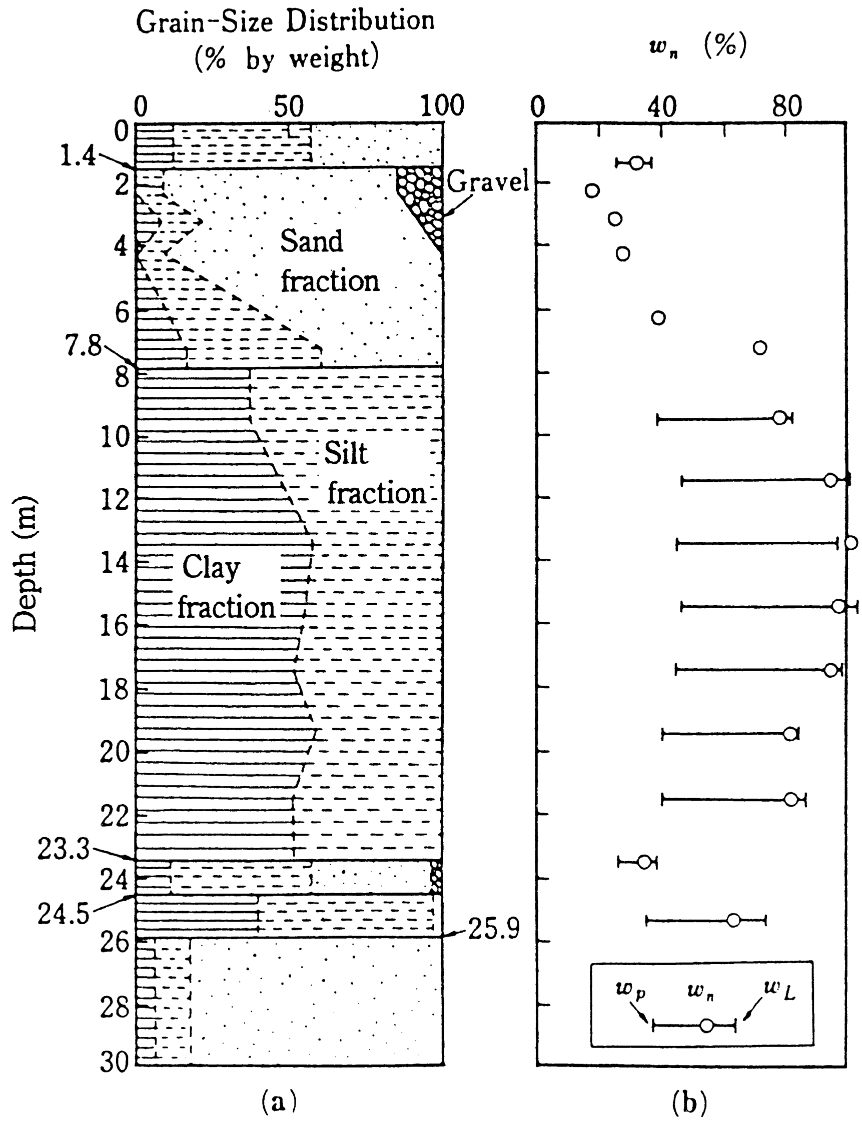

Fig. 16 Soil profile of Kanda Trial Embankment foundation (Japan Highway Public Corporation and Fudo Construction Co., Ltd.,1981).

Table 2 Soil parameters estimated by plasticity index (PI) for the Kanda Trial Embankment foundation.

SOIL	DEPTH(m)	PI	λ	κ	eo	Mc	Me	Konc	ν'
L-1	0- 1.4	11	(Elastic Material)						
L-2	1.4- 4.7	0	(Elastic Material)						
L-3	4.7- 7.8	0	(Elastic Material)						
L-4	7.8- 9.8	44	0.22	0.033	1.35	1.65	1.16	0.45	0.31
L-5	9.8-11.4	53	0.26	0.041	1.52	1.65	1.12	0.45	0.31
L-6	11.4-13.0	52	0.25	0.040	1.51	1.65	1.12	0.45	0.31
L-7	13.0-14.9	56	0.27	0.043	1.58	1.31	1.10	0.45	0.31
L-8	14.9-17.0	53	0.26	0.041	1.52	1.65	1.12	0.45	0.31
L-9	17.0-19.0	44	0.22	0.033	1.35	1.65	1.16	0.45	0.31
L-10	19.0-20.8	46	0.23	0.035	1.39	1.65	1.15	0.45	0.31
L-11	20.8-23.3	13	0.08	0.007	0.76	1.65	1.32	0.45	0.31
L-12	23.3-25.9	39	0.20	0.029	1.26	1.65	1.19	0.45	0.31

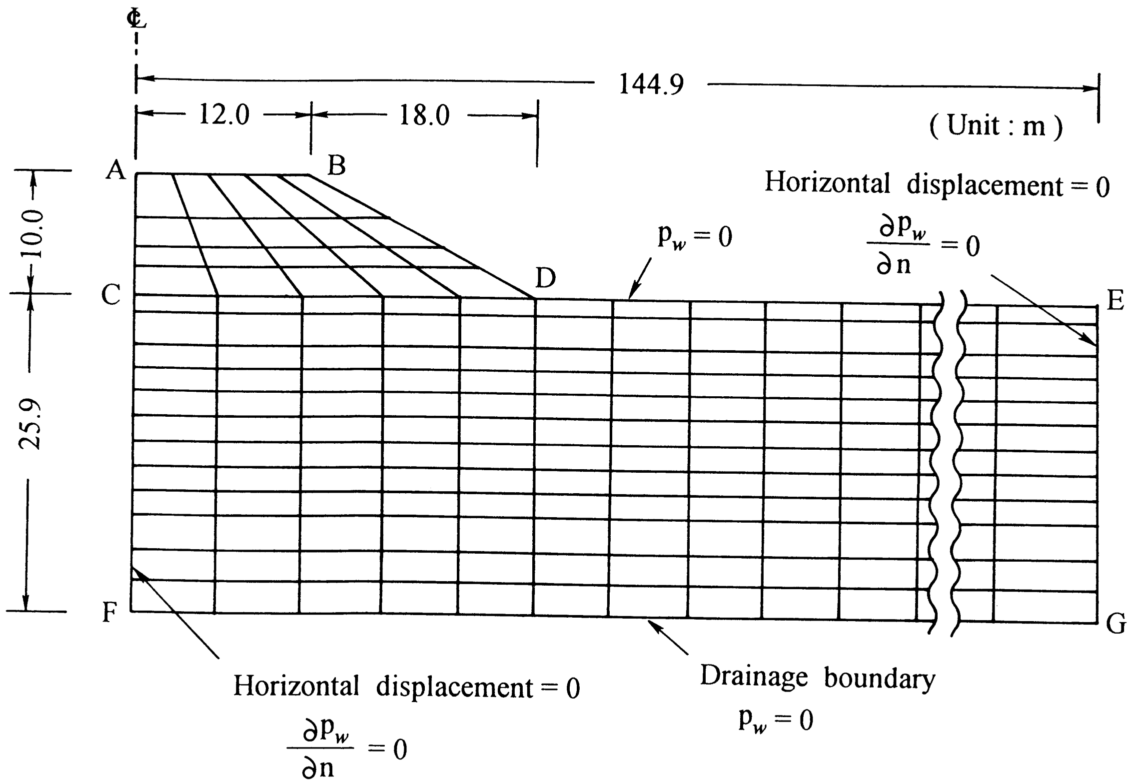

Fig. 17 The Finite Element Method mesh used in the study (Sakajo and Kamei, 1995).

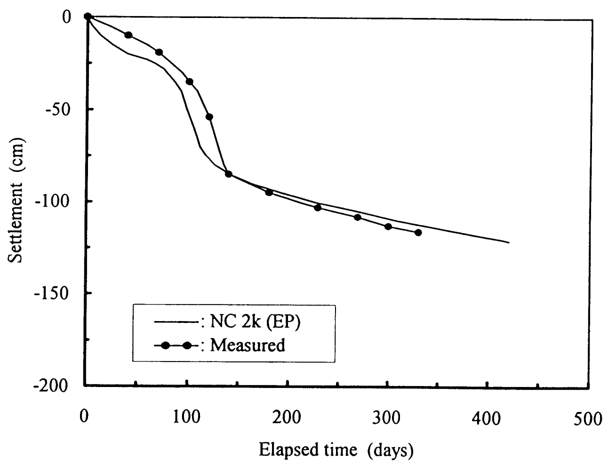

Fig. 18 Relationship between ground settlement and elapsed time at the ground surface (Sakajo and Kamei, 1995).

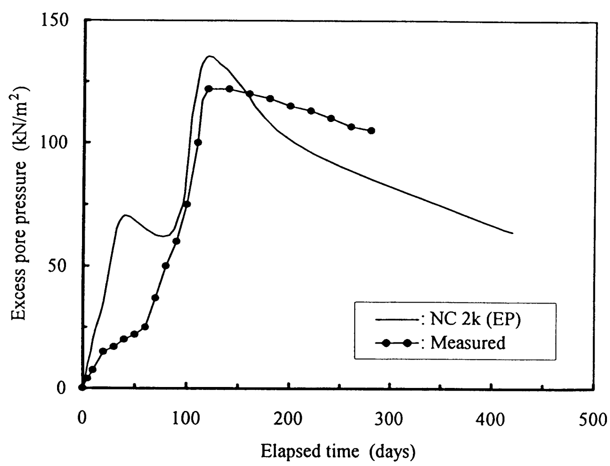

Fig. 19 Relationship between excess pore pressure and elapsed time at 21.5 m depth (Sakajo and Kamei, 1995).

and Sakajo, 1993) are found to be reasonable, and, therefore, the proposed method should be employed in engineering practice.

Conclusions

The following conclusions result from this study :

1) An attempt has been made to investigate the integrated mechanical behaviour of normally consolidated cohesive soils. It was examined by a series of triaxial tests on cohesive soils covering a wide range of plasticity indices, and centrifuge model tests on failure of embankments constructed on soils with plasticity index of 10 and 30.

2) Results of the triaxial tests show that strength anisotropy and strain anisotropy become more marked for soils with a lower plasticity index. In the

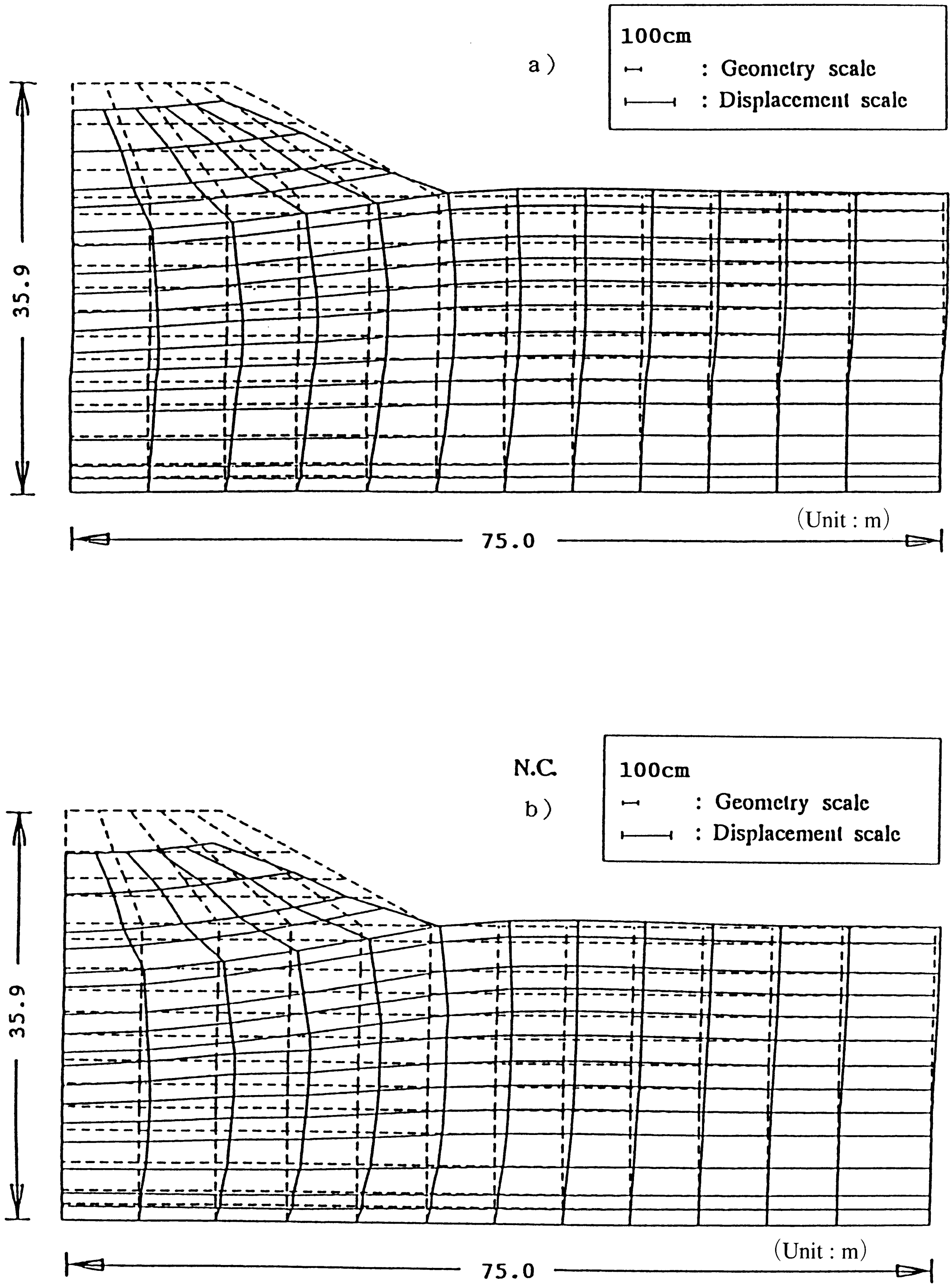

Fig. 20 Computed ground deformation (Sakajo and Kamei, 1995).
(a) At the completion of embankment construction
(b) 300 days since embankment construction commenced

centrifuge test, significant lateral deformation due to embankment loading was observed in soil with a plasticity index of 10. In addition, an attempt was made to provide some explanation for these results by Finite Element Method analysis.

3) The numerical method proposed by the author is a simple procedure which is able to predict the actual deformation of a deep clay foundation under an embankment with sufficient accuracy, although a number of simplifing assumptions have been made both in the soil parameters and the deformation analyses. It is , therefore, concluded that the proposed method may be utilized as a preliminary step in engineering practice.

Acknowledgments

The author would like to express his gratitude to Emeritus Professor A.Nakase of the Tokyo Institute of Technology, Professor T. Kimura of the Tokyo Institute of Technology, Professor O. Kusakabe of the Hiroshima University and Mr. H. Suzuki of the Ministry of Transport, for their keen interest and suggestions on this paper.

References

Basset, R. H. and Horner, J. N., 1979: Prototype deformations from centrifugal model tests, Proceedings, 7 th European Conference on Soil Mechanics and Foundation Engineering, Brighton, Vol.2, 1- 10.

Fukuda, T., 1983: Stability of embankments on clay , thesis presented to the Tokyo Institute of Technology, in partial fulfillment of the requirements for the degree of Master of Engineering(in Japanese).

Japan Highway Public Corporation and Fudo construction Co., Ltd., 1981: Report on Soil Improvement Construction in Kanda District of Joban High-way (in Japanese).

Kamei, T., 1985: A study on the mechanical behaviour of normally consolidated cohesive soils, thesis presented to the Tokyo Institute of Technology, in partial fulfillment of the requirements for the degree of Doctor of Engineering.

Kamei, T. and Sakajo, S., 1993: Settlement analysis of embankment foundation using elasto-viscoplastic model, Tuchi-to-Kiso, JSSMFE, Vol.41, No.2, 23-28(in Japanese).

Kurata, S. and Fujishita, T., 1961: Research on the engineering properties of sand-clay mixtures, Report of the Port and Harbour Research Institute, Yokosuka, Japan, 11(9), 389-424(in Japanese).

Mitchell, R. J., 1991: Centrifuge modelling as a consulting tool, Canadian Geotechnical Journal, Vol.28, No.1, 162-167.

Naganuma, M., Fukuda, T. Kusakabe, O. and Saitoh, K., 1983: Construction of embankments modeled in a geotechnical centrifuge, Proceedings, 17 th Japan National Conference on Soil Mechanics and Foundation Engineering, 843-844(in Japanese).

Nakase, A. and Kamei, T., 1983: Undrained shear strength anisotropy of normally consolidated cohesive soils, Soils and Foundations, 23(1), 91-101.

Nakase, A. and Kamei, T., 1984: Influence of anisotropy of deformation modulus on effective stress path, Soils and Foundations, 24(2), 106-110.

Nakase, A. and Kamei, T., 1988: Undrained shear strength of remoulded marine clays, Soils and Foundations, 28(1), 29-40.

Nakase, A., Kamei, T. and Kusakabe, O., 1988: Constitutive parameters estimated by plasticity index, J. Geotech.Engrg. Div., ASCE, 114(7),844-858.

Osterberg, J. O., 1978: Private correspondence with A. Nakase.

Schofield, A. N. and Wroth, C. P., 1968: Critical State Soil Mechanics, McGraw-Hill Book Co., London, England.

Sakajo, S. and Kamei, T., 1995: A simple procedure for evaluating deformation characteristics of deep clay foundation under embankment using elasto-plastic model, Proc. International Symposium on Compression and Consolidation of Clayey Soils at Hiroshima, Vol.1, 739-744.

Sekiguchi, H. and Ohta, H., 1977: Induced anisotropy and time dependency in clays, Proc.,9 th Int. Conf. on Soil Mechanics and Foundation Engineering, Specialty Session 9, Tokyo, Japan, 229-238.

Skempton, A. W., 1957: Discussion of "The planning and design of the new Hong Kong Air Port." Proc. Inst. Civ. Engrg., London, U. K., 7, 305-307.

（要　旨）

亀井健史，1995．正規圧密粘性土地盤の力学的挙動に関する総合的評価，島根大学地質学研究報告， 14.

従来不明な点が多かった中間土を含めた広範な粘性土の力学的挙動を要素試験・モデル実験から定量的に明らかにしている．また，極めて精度の高い室内土質試験結果に基づき筆者がすでに提案している土の弾粘塑性方程式に用いられる主要な土質定数を有限要素解析に適用することにより得られた結果は，要素試験・モデル試験結果をよく表現できることを示唆した．さらに，本解析手法の実務への応用と簡便な地盤変形解析手法を構築するため，標準貫入試験時に付随して得られる自然含水比とアッターベルグ限界試験に基づいた地盤のモデリングを提案し，多層軟弱粘性土地地盤の盛土に伴う盛土基礎地盤の変形解析を実施した．その結果，得られた解析結果と実測結果は非常によい対応性を示した．

以上要するに，地盤工学における室内試験・数値解析・実地盤挙動への適用といった一連の相互関係を総合的に解明している．